Received: *July 19, 1999*, Accepted: *October 14, 1999*

A collinear model for small-x physics*

Marcello Ciafaloni, Dimitri Colferai

Dipartimento di Fisica, Università di Firenze and INFN, Sezione di Firenze
Largo E. Fermi 2, 50125 Firenze, Italy
E-mail: Ciafaloni@fi.infn.it Colferai@fi.infn.it

Gavin P. Salam

INFN, Sezione di Milano
Via Celoria 16, 20133 Milano, Italy
E-mail: Gavin.Salam@mi.infn.it

Abstract: We propose a simple model for studying small-x physics in which we take only the collinearly enhanced part of leading and subleading kernels, for all possible transverse momentum orderings. The small-x equation reduces to a second order differential equation in $t \equiv \log k^2/\Lambda^2$ space, whose perturbative and strong-coupling features are investigated both analytically and numerically. For two-scale processes, we clarify the transition mechanism between the perturbative, non-Regge regime and the strong-coupling Pomeron behaviour.

Keywords: QCD, NLO Computations.

*Work supported by E.U. QCDNET contract FMRX-CT98-0194.

JHEP10(1999)017

Contents

1. Introduction

The problem of subleading logs corrections to the BFKL equation [1, 2, 3, 4] has been recently investigated by several authors [5]–[11] in connection with the small-x behaviour of structure functions and of two-scale processes [12, 13, 14].

We have advocated [8, 9, 11] in this context, the importance of incorporating Renormalisation Group (RG) improvements and collinear physics in a new form of the small-x equation. The latter has the virtue of including all collinearly enhanced higher order contributions to the kernel, and provides stable estimates of the resummed gluon anomalous dimension and of the hard Pomeron.

Here we present a simple, but powerful tool for studying the problem of small-x physics that we call *the collinear model* — namely a model where all and only the collinearly-enhanced physics is correctly included, in particular the full dependence on the one-loop running coupling, the splitting functions, and the so-called energy-scale terms [4, 8].

The model has the properties of correctly reproducing the one-loop renormalisation group results and of being symmetric (given a problem with two transverse scales, its results do not depend on which of the scales is larger). These are properties desired from the resummation of the NLL corrections in the case of the full BFKL kernel.

While it does not correctly resum the series of leading and subleading logarithms of s (i.e. the non-collinear part of the problem), in that region it does have a structure which qualitatively is very similar to that of the BFKL equation, and can usefully serve as a model. In contrast to the BFKL equation, it is very easily soluble, as a Schrödinger-like problem.

2. The collinear model

Let us start by recalling [4] that, in order to specify a small-x model for a hard process with two scales k and k_0, one should specify the energy scale s_0, the kernel and the impact factors. They all enter the $\boldsymbol{k}$-factorised form of the cross section

$$\sigma_{AB}(Y;k,k_0) = \int \frac{\mathrm{d}\omega}{2\pi\mathrm{i}} \left(\frac{s}{s_0(k,k_0)}\right)^{\omega} h_A(k)\, \mathcal{G}_\omega(k,k_0)\, h_B(k_0)\,, \tag{2.1}$$

where $Y \equiv \log s/s_0$ and

$$\mathcal{G}_\omega = \left[\omega - \mathcal{K}_\omega\right]^{-1} \tag{2.2}$$

is the gluon Green's function. In the following, we refer normally to the symmetrical factorised scale $s_0 = kk_0$, keeping in mind that for $k \gg k_0$ (or vice versa), one can switch to the relevant Bjorken variable k^2/s (or k_0^2/s) by the similarity transformation induced by $(k/k_0)^\omega$ on the kernel and the Green's function.

2.1 Definition of the model

Our collinear model is then defined — in logarithmic variables $t \equiv \log k^2/\Lambda^2$ — by specifying the kernel $\mathcal{K}_\omega(\alpha_\mathrm{s}(t),t,t')$ whose $\alpha_\mathrm{s}(t)$ expansion corresponds to higher and higher order collinear singular kernel for both $k \gg k'$ and $k' \gg k$.

In other words, our model is such that it reproduces the DGLAP limits [15] for branchings with ordered transverse momenta, and the anti-DGLAP limit for branchings with anti-ordered transverse momenta. Accordingly, the kernel governing a small-x branching of a gluon with transverse momentum k' into a gluon with transverse momentum k is (fig. 1)

$$\begin{aligned} \frac{1}{\omega}\mathcal{K}_\omega(t,t') &\equiv \frac{kk'}{\omega}\mathcal{K}_\omega(k,k') \\ &= \frac{\bar\alpha_\mathrm{s}(t)}{\omega}\exp\left\{-\frac{1+\omega}{2}(t-t') + A_1(\omega)\int_{t'}^{t}\bar\alpha_\mathrm{s}(\tau)\,\mathrm{d}\tau\right\}\Theta(t-t') + (t\leftrightarrow t')\,. \end{aligned} \tag{2.3}$$

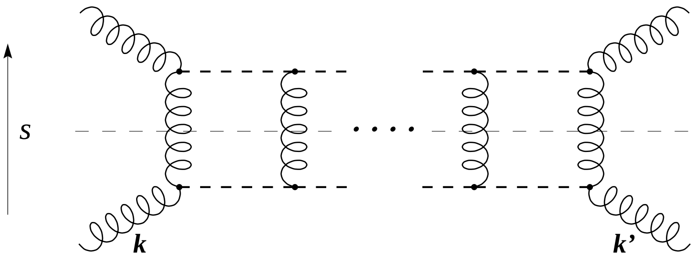

Figure 1: Subleading kernels being resummed by $\mathcal{K}_\omega(\boldsymbol{k}, \boldsymbol{k}')$ in eq. (2.3). Wavy (dashed) lines denote high-energy (low-energy) gluon exchanges, corresponding to the $\bar{\alpha}_\mathrm{s}/\omega$ ($A_1\bar{\alpha}_\mathrm{s}$) part of the gluon anomalous dimension.

The term proportional to $A_1(\omega)$ comes from the summation of the non-singular part of the DGLAP splitting function, including a full treatment of the running coupling:

$$\gamma_{gg}(\bar{\alpha}_\mathrm{s}, \omega) - \frac{\bar{\alpha}_\mathrm{s}}{\omega} = A_1(\omega)\bar{\alpha}_\mathrm{s}(t) + \mathcal{O}(\bar{\alpha}_\mathrm{s}^2)\,, \qquad \bar{\alpha}_\mathrm{s} \equiv \frac{N_c \alpha_\mathrm{s}}{\pi} = \frac{1}{bt}\,. \tag{2.4}$$

Therefore the kernel for a single small-x branching actually resums many branchings, of which the last (and only the last) is governed by the $1/\omega$ part of the splitting function.

The scale of $\bar{\alpha}_\mathrm{s}$ is the larger of the two scales involved in the branching, as implied by DGLAP. Finally, the factor kk' is due to the fact that we work in t-space instead of $\boldsymbol{k}$-space, and the remaining $\exp[-\frac{1}{2}\omega(t-t')]$ is due to the choice of scaling variable kk_0/s, as explained before.

The collinear properties of the kernel (2.3) can also be seen in γ-space, by the expansion

$$\mathcal{K}_\omega(k, k') = \sum_{n=0}^{\infty} [\bar{\alpha}_\mathrm{s}(k^2)]^{n+1}\; K_n^\omega(k, k')\,, \tag{2.5}$$

where the scale-invariant kernels K_n^ω have eigenfunctions $\mathrm{e}^{(\gamma-1/2)t}$ and eigenvalue functions $\chi_n^\omega(\gamma)$ given by [9]

$$\chi_n^\omega(\gamma) = \frac{1 \cdot A_1(A_1+b)\cdots(A_1+(n-1)b)}{(\gamma+\frac{1}{2}\omega)^{n+1}} + \frac{1\cdot(A_1-b)(A_1-2b)\cdots(A_1-nb)}{(1-\gamma+\frac{1}{2}\omega)^{n+1}}\,. \tag{2.6}$$

Of particular interest is the NL expansion

$$\begin{aligned}\int \mathrm{d}t'\; \mathcal{K}_\omega(t, t')\mathrm{e}^{-(\gamma-\frac{1}{2})(t-t')} &= \left(\bar{\alpha}_\mathrm{s}(t)\chi_0^\omega + \bar{\alpha}_\mathrm{s}(t)^2\chi_1^\omega\right) \qquad (2.7)\\ &\simeq \bar{\alpha}_\mathrm{s}(t)\left[\chi_0^0 - \frac{1}{2}\omega\left(\frac{1}{\gamma^2} + \frac{1}{(1-\gamma)^2}\right)\right] + \bar{\alpha}_\mathrm{s}(t)^2\chi_1^0 + \mathrm{NNL}\,,\end{aligned}$$

whose ω-dependence can be reabsorbed [11] in a redefinition of impact factors and kernel, to yield the leading and next-to-leading BFKL kernels of the model:

$$\begin{aligned}\chi_0 &= \frac{1}{\gamma} + \frac{1}{1-\gamma}\,,\\ \chi_1 &= \frac{A_1}{\gamma^2} + \frac{A_1 - b}{(1-\gamma)^2} - \frac{\chi_0}{2}\left(\frac{1}{\gamma^2} + \frac{1}{(1-\gamma)^2}\right)\,,\end{aligned} \tag{2.8}$$

where the renormalisation scale for $\bar{\alpha}_\mathrm{s}$ has been taken as t, i.e.

$$\mathcal{K}_\mathrm{BFKL}(\alpha_\mathrm{s}(t), \gamma) = \bar{\alpha}_\mathrm{s}(t)\chi_0(\gamma) + \bar{\alpha}_\mathrm{s}^2\chi_1(\gamma)\,.$$

At leading order, this reproduces the poles at $\gamma = 0$ and 1 of the true BFKL kernel. At next-to-leading order it reproduces the $\gamma = 0, 1$ quadratic and cubic poles of the true BFKL kernel. The leading order kernel differs from BFKL quite significantly numerically, but retains a very similar structure — a saddle point at $\gamma = 1/2$, implying a power growth of the cross section, and diffusion. The double and triple-polar part of the next-to-leading kernel turns out to be very close, even numerically, to the full BFKL NLO kernel, reproducing it to better than 7% over the whole range of γ from 0 to 1 (note though that this collinear kernel has single polar and other parts, so that as a whole it may not be quite this close to the full BFKL NLO kernel). This suggests that collinearly enhanced effects dominate the NLO kernel.

2.2 First order formulation

The main advantage of our collinear kernel from the point of view of this article is its relative simplicity. Specifically it can be written in factorised form:

$$\mathcal{K}_\omega(t, t') = U(t)\,V(t')\,\Theta(t - t') + U(t')\,V(t)\,\Theta(t' - t)\,, \tag{2.9}$$

where

$$\begin{aligned}U(t) &= \bar{\alpha}_\mathrm{s}(t)\exp\left\{-\frac{1+\omega}{2}t + A_1(\omega)\int^t \bar{\alpha}_\mathrm{s}(\tau)\,\mathrm{d}\tau\right\}\,,\\ V(t) &= \exp\left\{\frac{1+\omega}{2}t - A_1(\omega)\int^t \bar{\alpha}_\mathrm{s}(\tau)\,\mathrm{d}\tau\right\}\,.\end{aligned} \tag{2.10}$$

This allows us to recast the homogeneous BFKL equation,[1]

$$\omega\mathcal{F}(t) \equiv \omega k \mathcal{F}_\omega(k) = U(t)\int_{-\infty}^{t} \mathrm{d}t'\; V(t')\,\mathcal{F}(t') + V(t)\int_{t}^{\infty} \mathrm{d}t'\; U(t')\,\mathcal{F}(t') \tag{2.11}$$

[1]Since we work in t-space, the density $\mathcal{F}(t)$ differs by a factor of k from the customary [11] BFKL solution $\mathcal{F}(k)$, at scale kk_0.

as a differential equation. Dividing $\mathcal{F}$ into two parts,

$$\begin{aligned}\mathcal{A}(t) &= U(t)\int_{-\infty}^{t} \mathrm{d}t'\, V(t')\,\mathcal{F}(t') \\ \mathcal{B}(t) &= V(t)\int_{t}^{\infty} \mathrm{d}t'\, U(t')\,\mathcal{F}(t') \\ \omega\mathcal{F}(t) &= \mathcal{A}(t) + \mathcal{B}(t)\end{aligned} \tag{2.12}$$

and taking the derivative leads to a pair of coupled differential equations:

$$\begin{aligned}\frac{\mathrm{d}\mathcal{A}}{\mathrm{d}t} &= \frac{U'}{U}\mathcal{A} + UV\mathcal{F}\,, \\ \frac{\mathrm{d}\mathcal{B}}{\mathrm{d}t} &= \frac{V'}{V}\mathcal{B} - UV\mathcal{F}\,.\end{aligned} \tag{2.13}$$

For the specific kernel (2.3) that we consider, we have

$$\begin{aligned}\frac{\mathrm{d}\mathcal{A}}{\mathrm{d}t} &= \left(-\frac{1+\omega}{2} + A_1\bar{\alpha}_\mathrm{s} + \frac{\bar{\alpha}_\mathrm{s}'}{\bar{\alpha}_\mathrm{s}}\right)\mathcal{A} + \bar{\alpha}_\mathrm{s}\mathcal{F} \\ \frac{\mathrm{d}\mathcal{B}}{\mathrm{d}t} &= \left(\frac{1+\omega}{2} - A_1\bar{\alpha}_\mathrm{s}\right)\mathcal{B} - \bar{\alpha}_\mathrm{s}\mathcal{F}\end{aligned} \tag{2.14}$$

Since we have two coupled equations, there are two independent solutions. Examining the equation for large and positive t, where $\bar{\alpha}_\mathrm{s}$ is small, one sees that they can be classified as a regular solution

$$\mathcal{F}_R \sim \exp\left(-\frac{1+\omega}{2}t\right), \tag{2.15}$$

which is dominated by $\mathcal{A}$, and an irregular solution

$$\mathcal{F}_I \sim \exp\left(\frac{1+\omega}{2}t\right), \tag{2.16}$$

dominated by $\mathcal{B}$.

2.3 Second order formulation

The coupled set of differential equations (2.13) can be recast in the form of a simple second order equation for $\mathcal{F}$. In fact, by using (2.12), we can first rewrite (2.13) in the form

$$\omega\mathcal{F} = \left[\left(\partial_t - \frac{U'}{U}\right)^{-1} - \left(\partial_t - \frac{V'}{V}\right)^{-1}\right] UV\mathcal{F}\,. \tag{2.17}$$

Then, in order to eliminate the resolvents appearing in (2.17) we introduce the operator

$$\mathcal{D}_t = \left(\partial_t + \frac{U'}{U} - \frac{w'}{w}\right)\left(\partial_t - \frac{U'}{U}\right) = \left(\partial_t + \frac{V'}{V} - \frac{w'}{w}\right)\left(\partial_t - \frac{V'}{V}\right), \tag{2.18}$$

and the wronskian

$$w(t) = W[U,V] \equiv UV' - U'V = \bar{\alpha}_s(t)\left(1 + \omega - 2A_1\bar{\alpha}_s - \frac{\bar{\alpha}_s'}{\bar{\alpha}_s}\right). \qquad (2.19)$$

By applying $\mathcal{D}_t$ to (2.17) we finally obtain

$$\omega\mathcal{D}_t\mathcal{F} = \left(\frac{U'}{U} - \frac{V'}{V}\right) UV\mathcal{F} = -w(t)\mathcal{F}\,, \qquad (2.20)$$

which is the second order formulation that we were looking for.

Equation (2.20) can be recast in normal form by the similarity transformation

$$\mathcal{F} = \mathrm{const} \cdot \sqrt{w(t)}\, h(t)\,, \qquad (2.21)$$

which leads to a Schrödinger type equation,

$$(-\partial_t^2 + V_{\mathrm{eff}})\, h = 0 \qquad (2.22)$$

$$V_{\mathrm{eff}} = \frac{1}{4}\left(\frac{w'}{w}\right)^2 - \frac{1}{2}\left(\frac{w'}{w}\right)' - \frac{w}{\omega} + \frac{U''V' - V''U'}{w}\,. \qquad (2.23)$$

Note that the above derivation is valid for any form of the running coupling $\bar{\alpha}_s(t)$ which extrapolates the perturbative form $(bt)^{-1}$ into the strong coupling region around the Landau pole $t = 0$.

In what follows we consider various regularisations of the Landau pole, in particular:

$$\text{(a)} \qquad \bar{\alpha}_s(t) = \frac{1}{bt}\Theta(t - \bar{t}), \qquad \text{(cutoff case)}, \qquad (2.24)$$

$$\text{(b)} \qquad \bar{\alpha}_s(t) = \frac{1}{bt}\Theta(t - \bar{t}) + \frac{1}{b\bar{t}}\Theta(\bar{t} - t), \qquad \text{(frozen } \bar{\alpha}_s \text{ case)}, \qquad (2.25)$$

where $\bar{t} > 0$ sets the boundary of the perturbative behaviour.

It is obvious that such different regularisations will change the form of the potential (fig. 2) and thus the boundary conditions on $\mathcal{F}$ (or h) coming from the strong coupling region. A similar Schrödinger formulation was found [16] for the (Airy) diffusion model [17, 18] with running coupling, with a potential which roughly corresponds to the bottom of the well in fig. 2.

We consider in particular the solution $\mathcal{F}_R(t)$ ($\mathcal{F}_L(t)$) of the homogeneous equation (2.20) which is regular for $t \to +\infty$ ($t \to -\infty$). If both conditions are satisfied, $\mathcal{F}_R = \mathcal{F}_L$ is an eigenfunction of the BFKL equation. The pomeron singularity $\omega = \omega_{\mathbb{P}}$ is the maximum value of ω for which this occurs (ground state).

If $\omega > \omega_{\mathbb{P}}$, $\mathcal{F}_R \neq \mathcal{F}_L$ and the two solutions have rather different features. Due to the locality of the differential equation, $\mathcal{F}_R$ is *independent* of the regularisation in the region $t > \bar{t}$. On the other hand, $\mathcal{F}_L$ will be dependent on the behaviour of $\bar{\alpha}_s(t)$ for

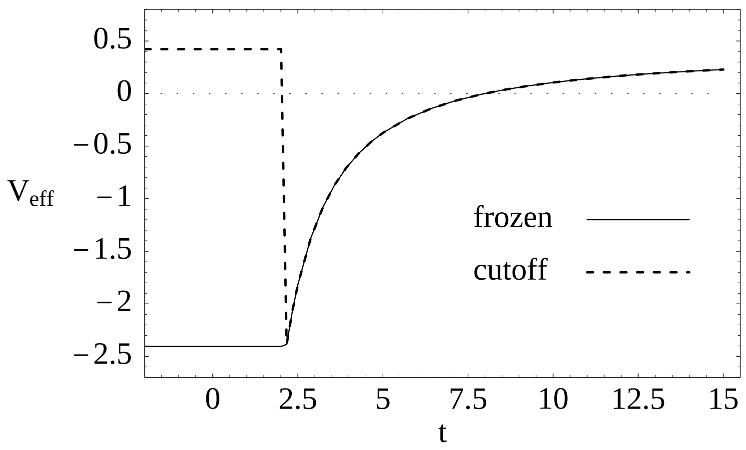

Figure 2: Qualitative t-dependence of the effective potential for the regularisations of type (a) and (b) of the coupling strength.

$t < \bar{t}$. For instance, in the case of $\bar{\alpha}_{\rm s}(t)$ being frozen (2.25), $\mathcal{F}_L$ has the exponential behaviour

$$\mathcal{F}_L(t) \sim {\rm e}^{\kappa t}\,, \qquad (t < \bar{t})\,, \tag{2.26}$$

where $\kappa = \sqrt{V_{\rm eff}(t < \bar{t})}$ is found from (2.23) to be

$$\kappa^2 = \left[\frac{1}{2}(1+\omega) - A_1\bar{\alpha}_{\rm s}(\bar{t})\right]\left[\frac{1}{2}(1+\omega) - A_1\bar{\alpha}_{\rm s}(\bar{t}) - \frac{2\bar{\alpha}_{\rm s}(\bar{t})}{\omega}\right]. \tag{2.27}$$

On the other hand, if $\bar{\alpha}_{\rm s}(t)$ is cutoff, it is simpler to use directly the first-order formulation, (2.13). We note that we can write

$$\omega\mathcal{F}_L = \mathcal{A}_L + \mathcal{B}_L = \bar{\alpha}_{\rm s}(t)a_L(t) + \mathcal{B}_L(t)\,, \tag{2.28}$$

where a_L and $\mathcal{B}_L$ are *continuous* at $t = \bar{t}$, and are exponentially behaved, $a_L \sim \mathcal{B}_L \sim \exp(\frac{1}{2}(1+\omega)t)$, for $t < \bar{t}$. By using (2.14) we then obtain

$$\left.\frac{\mathcal{A}_L}{\bar{\alpha}_{\rm s}(t)}\right|_{t=\bar{t}_+} = a_L(\bar{t}) = \frac{\mathcal{B}_L(\bar{t})}{\omega(1+\omega)}, \tag{2.29}$$

which defines the boundary condition for the $\mathcal{A}_L$ and $\mathcal{B}_L$ components of $\mathcal{F}_L$ in this case.

2.4 Factorisation of non-perturbative effects

The basic tool for describing BFKL evolution is the Green's function $\mathcal{G}_\omega(t,t_0) \equiv kk_0\mathcal{G}_\omega(k,k_0)$, which satisfies the inhomogeneous small-x equation

$$\omega\mathcal{G}_\omega(t,t_0) = \delta(t-t_0) + \mathcal{K}_\omega \otimes \mathcal{G}_\omega(t,t_0), \tag{2.30}$$

and is supposed to be well-behaved for $t, t_0 \to \pm\infty$. The problem of factorisation is the question of the (in)dependence on the non-perturbative strong-coupling region.

For $t \neq t_0$, $\mathcal{G}_\omega$ satisfies the same differential equation as $\mathcal{F}$ and is thus a superposition of two independent solutions. The large-t behaviour implies a regularity condition and suggests the expression

$$\mathcal{G}_\omega(t,t_0) = \mathcal{F}_R(t)\mathcal{F}_L(t_0)\Theta(t-t_0) + \mathcal{F}_L(t)\mathcal{F}_R(t_0)\Theta(t_0-t)\,, \qquad (t \neq t_0) \tag{2.31}$$

where $\mathcal{F}_R$ ($\mathcal{F}_L$) is the regular solution for $t \to +\infty$ ($t \to -\infty$) defined in the previous subsection.

Actually (2.31) is a rigorous consequence of the second-order formulation. In fact, $\mathcal{G}_\omega$ satisfies the differential equation

$$\left(\mathcal{D}_t + \frac{w}{\omega}\right)\mathcal{G}_\omega = \frac{1}{\omega}\mathcal{D}_t\delta(t-t_0)\,. \tag{2.32}$$

With a little thought, one can realize that $\mathcal{G}_\omega$ must contain a delta function term in the form

$$\mathcal{G}_\omega(t,t_0) = \frac{1}{\omega}\delta(t-t_0) + \hat{\mathcal{G}}_\omega(t,t_0) \tag{2.33}$$

and hence

$$\left(\mathcal{D}_t + \frac{w}{\omega}\right)\hat{\mathcal{G}}_\omega = -\frac{w}{\omega^2}\delta(t-t_0) \tag{2.34}$$

showing that $\hat{\mathcal{G}}$ is continuous function at $t = t_0$ with discontinuous derivative. Eq. (2.34) is an inhomogeneous Schrödinger type equation with a delta source, and its solution can be found in standard textbooks to be just like the RHS of eq. (2.31) also for $t = t_0$. We conclude that

$$\mathcal{G}(t,t_0) = \frac{1}{\omega}\delta(t-t_0) + \mathcal{F}_R(t)\mathcal{F}_L(t_0)\Theta(t-t_0) + \mathcal{F}_L(t)\mathcal{F}_R(t_0)\Theta(t_0-t) \tag{2.35}$$

with the normalisation

$$\mathcal{F}_{R,L}(t) = \frac{\sqrt{w(t)}}{\omega}h_{R,L}(t), \qquad W[h_R,h_L] \equiv h_R h_L' - h_R' h_L = 1\,. \tag{2.36}$$

The main consequence of (2.31) is that the regularisation dependence is factorised away in $\mathcal{F}_L$, whenever t or t_0 are large enough. This happens in particular in the collinear limit $t - t_0 \gg 1$ relevant for structure functions.

3. Solutions: analytical features

The collinear model just defined can be solved in principle as a Schrödinger problem by known analytical and numerical techniques and for both types of solutions occurring in the Green's function (2.2) (i.e., the left-regular and the right-regular ones).

The regular solution $\mathcal{F}_R$ is, for large t, perturbative, i.e., independent of the potential in the strong coupling region $t \leq \bar{t}$, while the left-regular one $\mathcal{F}_L$ is dependent on the strong coupling boundary conditions through a reflection coefficient $S(\omega)$, which occurs in its expression for $t > \bar{t}$:

$$\mathcal{F}_L(t) = \mathcal{F}_I(t) + S(\omega)\mathcal{F}_R(t)\,, \tag{3.1}$$

where $\mathcal{F}_R$ ($\mathcal{F}_I$) denote the regular (irregular) solution for $t > \bar{t}$, with the relative normalisation $W[h_R, h_I] = 1$.

The coefficient $S(\omega)$ is formally found from the continuity of the relevant logarithmic derivatives at $t \geq \bar{t}_+$, as in the familiar Schrödinger case, i.e.,

$$S(\omega) = \frac{\mathcal{F}_I(\bar{t}_+)}{\mathcal{F}_R(\bar{t}_+)} \cdot \frac{\mathcal{L}_I(\omega) - \mathcal{L}_L(\omega)}{\mathcal{L}_L(\omega) - \mathcal{L}_R(\omega)}\,, \qquad \mathcal{L}_i \equiv \frac{\dot{\mathcal{F}}_i(\bar{t}_+)}{\mathcal{F}_i(\bar{t}_+)} \tag{3.2}$$

The coefficient $\mathcal{L}_L$ is provided by the strong coupling boundary conditions. From eqs. (2.26), (2.14) and (2.29) we find

$$\mathcal{L}_L|_{\text{freezing}} = \kappa(\omega) \tag{3.3}$$

$$\mathcal{L}_L|_{\text{cutoff}} = \left[\left(\frac{1+\omega}{2} - A_1\bar{\alpha}_s(\bar{t})\right)\left(1 - \frac{\bar{\alpha}_s(\bar{t})}{\omega(1+\omega)}\right) + \frac{\bar{\alpha}_s'(\bar{t})}{\omega(1+\omega)}\right]\left(1 + \frac{\bar{\alpha}_s(\bar{t})}{\omega(1+\omega)}\right)^{-1}, \tag{3.4}$$

where $\bar{\alpha}_s(\bar{t})$ denotes the $t = \bar{t}_+$ value of $\bar{\alpha}_s$. Recall that in the cut-off case, the $\mathcal{F}_L$ solution dies out rapidly $\sim \exp\frac{1}{2}(1+\omega)(t-\bar{t})$ in the $t < \bar{t}$ region (cf. sect. 2.3).

Let us remark that, while $\mathcal{F}_I$ and $\mathcal{F}_R$ are expected to have an essential singularity at $\omega = 0$ only, (cf. sect. 3.3), the coefficient $S(\omega)$ displays the leading part of the ω-spectrum in $\Re(\omega) > 0$, and in particular the leading Pomeron singularity $\omega_{\mathbb{P}}$. In the frozen α_s case the spectrum is just a continuum occurring in $\kappa(\omega)$ itself, while in the cut-off case we expect poles at ω-values such that $\mathcal{L}_L(\omega) = \mathcal{L}_R(\omega)$, both being analytic functions in $\Re(\omega) > 0$. Mixed cases are also possible, depending on the detailed shape of the potential in the strong coupling region.

Eq. (3.1) allows us to rewrite the Green's function for $t > t_0$ and $\omega > \omega_{\mathbb{P}}$ in terms of $S(\omega)$ in eq. (3.2) as follows:

$$\mathcal{G}_\omega(t, t_0) = \mathcal{F}_R(t)\left[\mathcal{F}_I(t_0) + S(\omega)\mathcal{F}_R(t_0)\right]\,. \tag{3.5}$$

If both $t, t_0 \gg 1$, but $t - t_0 = \mathcal{O}(1)$, eq. (3.5) is dominated by the first term, the second being suppressed exponentially in t_0 because the regular solution is much smaller than the irregular one for $t_0 \gg 1$. This term is, on the other hand, defined by boundary conditions for $t, t_0 \to +\infty$ only, and is therefore independent of the strong coupling region. Its analytical and numerical form will be discussed in more detail in the following.

The second term in eq. (3.5) carries the regularisation dependence and contains the leading ω-singularities, in particular $\omega_{\mathbb{P}}$ (ref. [16]). In $Y \equiv \log(s/kk_0)$ space, the sum in eq. (3.5) defines two asymptotic regimes, as we shall see.

3.1 Perturbative regime: ω-expansion and WKB limit

Approximate homogeneous solutions in the large-t region can be found, as in the full small-x equation, by the method of the γ-representation and ω-expansion. The regular solution is approximated, for $\omega \ll 1$, by the expression:

$$\mathcal{F}_R(t) \simeq \int \frac{\mathrm{d}\gamma}{2\pi \mathrm{i}} \exp\left[\left(\gamma - \frac{1}{2}\right) t - \frac{X^\omega}{b\omega}\right] , \tag{3.6}$$

with

$$\partial_\gamma X^\omega \equiv \chi(\gamma, \omega) = \chi_0^\omega(\gamma) + \omega \frac{\chi_0^\omega(\gamma)}{\chi_1^\omega(\gamma)} + \mathcal{O}(\omega^2) \tag{3.7}$$

where, for the collinear model,

$$\begin{aligned} \chi_0^\omega(\gamma) &= \frac{1}{\gamma + \frac{1}{2}\omega} + \frac{1}{1 - \gamma + \frac{1}{2}\omega} , \\ \chi_1^\omega(\gamma) &= \frac{A_1}{(\gamma + \frac{1}{2}\omega)^2} + \frac{A_1 - b}{(1 - \gamma + \frac{1}{2}\omega)^2} . \end{aligned} \tag{3.8}$$

In [11] this representation was extensively studied, and shown to be a solution of the problem up to next-to-leading order in ω and to all orders for the collinear structure. But this was only guaranteed to work true for small values of ω (whereas for the continuation with the DGLAP anomalous dimensions it is useful to be able to access high ω as well). Also there was no way of determining the coefficient of any higher-order error introduced by the procedure. A comparison of this representation with the exact solution, as is possible in the collinear model, is therefore important (cf. sect. 4.1).

The expressions (3.6)–(3.8) can be further specialised in the large-t limit, where (3.6) is dominated by a saddle point at $\gamma = \bar{\gamma}$:

$$b\omega t = \chi(\bar{\gamma}, \omega) . \tag{3.9}$$

The latter is related to the WKB approximation for solving the differential equation (2.22). In fact, on the basis of eqs. (2.22) and (2.36), one can prove the asymptotic expansion

$$\mathcal{F}_R(t) = \frac{1}{\omega} \sqrt{\frac{w(t)}{2\,\kappa(t)}} \exp\left\{ - \int^t \kappa(\tau)\, \mathrm{d}\tau \right\} \times \left[1 + \mathcal{O}\left(\frac{1}{t}\right)\right] , \tag{3.10}$$

where $\kappa(t)$ is defined in terms of the effective potential (2.23) as

$$\kappa^2(t) \equiv V_{\text{eff}}(t) = \frac{1}{2}\left(1 + \omega - \frac{2A_1 - b}{bt}\right)\left[\frac{1}{2}\left(1 + \omega - \frac{2A_1 - b}{bt}\right) - \frac{2}{b\omega t}\right] + \mathcal{O}\left(\frac{1}{t^2}\right) \tag{3.11}$$

and is related to the saddle point value $\bar{\gamma}(\omega, t)$ of eq. (3.9) by

$$\bar{\gamma} = \frac{1}{2}\left(1 + \frac{1}{t}\right) - \kappa(t) + \mathcal{O}\left(\frac{1}{t^2}\right) . \tag{3.12}$$

It is interesting to note that in the collinear model, because of the differential equation (2.22), the present method yields the irregular solution also, which is obtained by just changing the sign of the WKB momentum $\kappa(t)$, i.e.,

$$\mathcal{F}_I(t) = \frac{1}{\omega}\sqrt{\frac{w(t)}{2\,\kappa(t)}} \exp\left\{+\int^t \kappa(\tau)\,\mathrm{d}\tau\right\} . \tag{3.13}$$

This is useful for evaluating the Green's function which according to eqs. (3.5), (3.10) and (3.13) takes the form

$$\mathcal{G}_{\mathrm{WKB}}(t, t_0) = \frac{1}{2\omega^2}\sqrt{\frac{w(t)w(t_0)}{\kappa(t)\kappa(t_0)}}\left[\exp\left\{-\int_{t_0}^t \kappa(\tau)\,\mathrm{d}\tau\right\} + \right. \tag{3.14}$$

$$\left. + S(\omega)\exp\left\{-\left(\int_{t_s}^{t_0} + \int_{t_s}^{t}\right)\kappa(\tau)\,\mathrm{d}\tau\right\}\right], \quad (t > t_0)\,,$$

where t_s is the zero of κ and $S(\omega)$ has to be determined from the boundary conditions on $\mathcal{F}_L$ at $t = \bar{t}$, as explained in eq. (3.2).

3.2 Strong-coupling features

For intermediate, small, and negative t's, the collinear model enters a second regime, where both kinds of solutions oscillate. Given the definitions of the effective potential in (2.23), the regime's boundary is roughly given by $t < \chi_m / b\omega$, where $\kappa(t)$ becomes negative, and χ_m is the minimum (in γ) of the effective eigenvalue function $\chi(\gamma, \omega)$ defined in eq. (3.7).

A basic question concerning this regime is the spectrum of $\mathcal{K}_\omega$, which provides the ω-singularities of the Green's function, which are embodied in $S(\omega)$, and in turn determine the high-energy behaviour of the cross section.

The leading ω-singularity is the Pomeron $\omega_{\mathbb{P}}$, i.e., the maximum ω value for which $\mathcal{F}_L$ and $\mathcal{F}_R$ match each other, providing a zero energy bound state in the potential (2.23). The Pomeron properties are dependent on the strong coupling boundary conditions which are basically the frozen α_{s} and cut-off cases already considered in sect. 2.

The first case is fairly simple, because of the fixed value of $\bar{\alpha}_{\mathrm{s}}$ for $t < \bar{t}$. In this region, because of the replacement

$$\exp\left\{A_1(\omega)\int_{t'}^{t}\bar{\alpha}_{\mathrm{s}}(\tau)\,\mathrm{d}\tau\right\} \to \mathrm{e}^{\bar{\alpha}_{\mathrm{s}}A_1(\omega)(t-t')}$$

the solution is a plane wave whose momentum $\kappa(\omega)$ is given in eq. (2.27) and occurs in the S-matrix expressions (3.2) and (3.3). Therefore, $\omega_{\mathbb{P}}$ defines the boundary of the continuum spectrum, given by $\kappa(\omega) = 0$, or

$$\omega_{\mathbb{P}} = \frac{4\bar{\alpha}_{\mathrm{s}}}{1 + \omega_{\mathbb{P}} - 2\bar{\alpha}_{\mathrm{s}} A_1} \,. \tag{3.15}$$

This is to be compared with the saddle point definition of the hard Pomeron [11] $\omega_s(\bar{t})$, which is obtained by minimising the solution (as a function of γ) of

$$\omega_s = \bar{\alpha}_{\mathrm{s}} \left(\chi_0^{\omega_s}(\gamma) + \omega_s \frac{\chi_1^{\omega_s}}{\chi_0^{\omega_s}} \right) \,. \tag{3.16}$$

Taking the $b = 0$ form for χ_1^{ω} the minimum is at $\gamma = 1/2$, and ω_s is given by

$$\omega_s = \frac{4\bar{\alpha}_{\mathrm{s}}}{1 + \omega_s - 2\bar{\alpha}_{\mathrm{s}} A_1} \,. \tag{3.17}$$

which is identical to the true $\omega_{\mathbb{P}}$.

In [11] a second critical ω-exponent was proposed, termed ω_c, corresponding to the position of the rightmost singularity of the anomalous dimension of the integrated gluon distribution. In the collinear model the integrated gluon distribution can be defined as

$$g_\omega(t) = \int_{-\infty}^{t} \mathrm{d}t' \, \exp\left[-\frac{1+\omega}{2}(t-t') + A_1 \int_{t'}^{t} \mathrm{d}\tau \, \bar{\alpha}_{\mathrm{s}}(\tau) \right] \mathcal{F}(t') = \frac{1}{\bar{\alpha}_{\mathrm{s}}(t)} \mathcal{A}(t) \,, \tag{3.18}$$

because the corresponding density (at energy-scale k^2) $\mathrm{e}^{\frac{1+\omega}{2}t} g_\omega(t)$ can be shown to satisfy, in the collinear limit, the usual DGLAP equation with anomalous dimension $(1/\omega + A_1)\bar{\alpha}_{\mathrm{s}}$. The singularity of the effective anomalous dimension (at scale k^2)

$$\gamma_{\mathrm{eff}}(\alpha_{\mathrm{s}}(t), \omega) \equiv \frac{\mathrm{d}}{\mathrm{d}t} \ln g_\omega(t) + \frac{1+\omega}{2} \tag{3.19}$$

is at the point $\omega = \omega_c(t)$ where $g_\omega(t)$ goes to zero, i.e., where $\mathcal{A}(t)$ goes to zero.

This critical exponent ω_c is related to $\omega_{\mathbb{P}}$ for the cutoff case, in which $\alpha_{\mathrm{s}}(t) = 0$ for $t < \bar{t}$. In fact, since $\mathcal{A}(t) \sim \bar{\alpha}_{\mathrm{s}}(t)$, we have $\mathcal{A} = 0$ for $t < \bar{t}$; but we noticed in sect. 2 that $\mathcal{A}(t)/\bar{\alpha}_{\mathrm{s}}(t) \sim g_\omega(t)$ is instead continuous at $t = \bar{t}$, so that for $t \to \bar{t}_+$, $\omega_{\mathbb{P}}$ satisfies the boundary condition

$$\mathcal{A}(\bar{t}_+) = \bar{\alpha}_{\mathrm{s}}(\bar{t}_+) \frac{\mathcal{B}(\bar{t})}{\omega_{\mathbb{P}}(1 + \omega_{\mathbb{P}})} \neq 0 \,. \tag{3.20}$$

This means that $\omega_c(\bar{t}) < \omega_{\mathbb{P}}$, because the depth of the well, determined by $\omega < \omega_s(\bar{t})$, is to be further decreased below $\omega_{\mathbb{P}}$ in order to have $\mathcal{A}(\bar{t}_+) = 0$.

The relationships just found ($\omega_{\mathbb{P}}^{\mathrm{freezing}} = \omega_s(\bar{t})$, $\omega_{\mathbb{P}}^{\mathrm{cutoff}} > \omega_c(\bar{t})$) represent two extreme cases of the boundary condition dependence of $\omega_{\mathbb{P}}$. If the coupling $\bar{\alpha}_{\mathrm{s}}(t) > 0$ is positive but has intermediate size and shape for $t < \bar{t}$, we expect in general that

$$\omega_c(\bar{t}) < \omega_{\mathbb{P}} < \omega_s(\bar{t}) \,, \tag{3.21}$$

i.e., the lower and upper bounds mentioned in ref. [11].

3.3 High energy behaviour and diffusion

It is widely believed that a two-scale process — described by a small-x equation of BFKL type — is perturbative for large enough t and t_0, while it becomes a strong coupling process if the energy is so large as to allow diffusion to small values of $t \simeq 0$ ($k^2 \simeq \Lambda^2$) [20, 19].

In the collinear model the Green's function has the explicit expression (3.5), in which the strong-coupling information is clearly embodied in the reflection coefficient $S(\omega)$. Therefore it allows a direct study of the relative importance of the "perturbative" part $\mathcal{F}_R \otimes \mathcal{F}_I$ and of the "strong-coupling" part $S\, \mathcal{F}_R \otimes \mathcal{F}_R$, induced by diffusion through the boundary conditions at $t = \bar{t}$.

For large t and t_0, $\mathcal{G}_\omega$ takes the approximate WKB form (3.14), that we study in the special case $t = t_0$, so that

$$\mathcal{G}(Y;t,t) \simeq \int \frac{\mathrm{d}\omega}{2\pi\mathrm{i}}\, \mathrm{e}^{\omega Y} \frac{w(t)}{2\omega^2 \kappa_\omega(t)} \left[1 + S(\omega) \exp\left(-2\int_{t_s}^{t} \kappa_\omega(\tau)\, \mathrm{d}\tau\right)\right], \tag{3.22}$$

provided $\int_{t_s}^{t} \kappa_\omega(\tau)\, \mathrm{d}\tau \gg 1$.

We now notice that if $Y = \log(s/kk_0) = \log s/\Lambda^2 - t \gg 1$ is not too large, the first term in the expression (3.22) is characterised by a shallow saddle point at $\omega = \bar{\omega}$, such that

$$Y = \frac{1}{2}\frac{\partial}{\partial\omega} \log \kappa^2 \bigg|_{\bar{\omega}} \simeq \frac{bt}{2\,(b\bar{\omega}t - \chi_m)}\,, \tag{3.23}$$

and therefore

$$\bar{\omega}(Y,t) \simeq \omega_s(t) + \frac{1}{2Y} = \frac{\chi_m}{bt} + \frac{1}{2Y}\,, \qquad \chi_m = 4\left(1 + \omega_s - \frac{2A_1 - b}{bt}\right)^{-1}. \tag{3.24}$$

so that $\bar{\omega}(Y,t)$ is not much different from $\omega_s(t)$, the saddle point exponent mentioned before (eq. (3.16)). Furthermore, at this saddle point the phase function takes the value ($\chi_m'' \simeq \chi_m^3/2$)

$$\int_{t_s}^{t} \kappa(\tau)\, \mathrm{d}\tau \simeq \sqrt{\frac{2}{\chi_m''}} \int_{t_s}^{t} (b\bar{\omega}\tau - \chi_m)^{1/2}\, \mathrm{d}\tau \simeq \frac{t}{3\chi_m \sqrt{\chi_m''}} \left(\frac{bt}{Y}\right)^{3/2} \gg 1\,, \tag{3.25}$$

provided

$$bt \sim \omega_s^{-1} \ll 2Y \ll \left(\frac{4}{3b}\right)^{2/3} \omega_s^{-5/3} \sim \alpha_\mathrm{s}^{-5/3}\,. \tag{3.26}$$

In other words, the saddle point (3.24) is self consistent, i.e., it exists in the WKB region of eq. (3.25), provided the effective parameter $\alpha_\mathrm{s}^{5/3} Y \ll 1$.

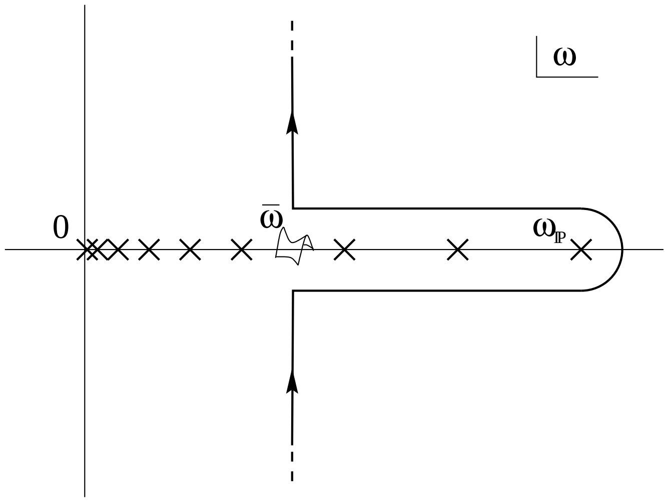

Figure 3: The contour of integration for the Green's function $\mathcal{G}_\omega(Y;t,t)$, displaying the pole contribution and the background integral along the imaginary axis.

The actual evaluation of (3.22) is now performed by distorting the ω contour as in fig. 3 and picking up the background integral around the saddle-point (3.23) and the ω-poles:

$$\mathcal{G}(Y;t,t) \simeq \frac{1}{\sqrt{2\pi\chi''_m \bar{\alpha}_\mathrm{s} Y}}\, \mathrm{e}^{\omega_s(t)Y} \times \left[1 + \mathcal{O}(\alpha_\mathrm{s}^5 Y^3)\right] + \mathrm{e}^{\omega_\mathbb{P} Y} R_\mathbb{P} \mathrm{e}^{-(1+\omega_\mathbb{P})t} \,. \tag{3.27}$$

Here we have kept the leadingPomeron pole, with residue $R_\mathbb{P}$, and neglected the nearby poles $\omega_n \gtrsim \bar{\omega} = \omega_s + 1/2Y$, which are anyhow exponentially suppressed because of the large phase function $\mathcal{O}\left((\alpha_\mathrm{s}^5 Y^3)^{-1/2}\right)$ of eq. (3.25).[2] Note the exponential suppression factor of the Pomeron contribution which, for large t values, comes from evaluating the second term in (3.22) with $\kappa(\omega_\mathbb{P}) \simeq (1+\omega_\mathbb{P})/2$. Note also that the background contribution is evaluated by the integral

$$\int_{\epsilon - \mathrm{i}\infty}^{\epsilon+\mathrm{i}\infty} \frac{\mathrm{d}x}{2\mathrm{i}\sqrt{\pi x}} \mathrm{e}^x = 1 \,, \qquad (x \equiv (\omega - \omega_s)Y) \tag{3.28}$$

rather than by naïve quadratic fluctuations around $x = 1/2$.

The corrections to eq. (3.22), depending on the (small) parameter $\alpha_\mathrm{s}^5 Y^3$, can be explicitly evaluated from higher order WKB terms. More simply, we can use the fact that the effective ω values are close to the minimum of χ, in order to use the Airy form [16] of the Green's function, which in the cutoff case is given by the expression

$$\mathcal{G}_\omega(t,t_0) = \pi \frac{t_0}{\omega} \left(\frac{2b\omega}{\chi''_m}\right)^{2/3} \mathrm{Ai}(\xi) \left[\mathrm{Bi}(\xi_0) - \frac{\mathrm{Bi}(\bar{\xi})}{\mathrm{Ai}(\bar{\xi})} \mathrm{Ai}(\xi_0)\right] , \tag{3.29}$$

[2]Of course, the background integral contribution is equivalent to the one of the poles $\omega_n \lesssim \bar{\omega}$, as can be seen by displacing the contour further to the left.

where the variables

$$\xi = \left(\frac{2b\omega}{\chi_m''}\right)^{1/3}\left(t - \frac{\chi_m}{b\omega}\right), \qquad \bar{\xi} = -\left(\frac{2b\omega}{\chi_m''}\right)^{1/3}\left(\frac{\chi_m}{b\omega} - \bar{t}\right), \tag{3.30}$$

evaluated at $\omega \simeq \bar{\omega}$, turn out to be both large parameters $\sim t^{2/3}$ of opposite sign. By using the expansion (based on results in [21])

$$\mathrm{Ai}(\xi)\mathrm{Bi}(\xi) \simeq \frac{1}{2\pi\sqrt{\xi}}\sum_{n=0}^{\infty}\frac{c_{3n}}{\xi^{3n}}, \qquad c_{3n} = \frac{1}{2^{8n}\,3^n}\frac{(6n)!}{n!\,(3n)!}, \tag{3.31}$$

and the saddle-point value

$$\xi^{\frac{3}{2}}(\bar{\omega}, t) \simeq \sqrt{\frac{2}{\chi_m''}\frac{t}{\chi_m}}\left(\frac{bt}{2Y}\right)^{3/2},$$

we see that the correction is indeed of order $\bar{\alpha}_s^5 Y^3$. The quantitative evaluation requires an expansion in inverse powers of $x = (\omega - \omega_s)Y$. Using eq. (3.31) and the integrals

$$\int_{\epsilon - \mathrm{i}\infty}^{\epsilon + \mathrm{i}\infty} \frac{\mathrm{d}x}{2\mathrm{i}\sqrt{\pi x}}\, x^{-k}\mathrm{e}^{x} = \frac{2^{2k}\,k!}{(2k)!},$$

we finally obtain, for the perturbative part of the Green's function (3.27) the sub-asymptotic correction factor

$$\sum_{n=0}^{\infty}\frac{1}{n!}\left(\frac{\omega_s^2\chi_m'' Y^3}{24bt^3}\right)^n = \exp\left(\frac{\chi_m^2\chi_m'' b^2\,\bar{\alpha}_s^5 Y^3}{24}\right). \tag{3.32}$$

The latter turns out to coincide with the "non-Regge correction" to the "Regge exponent" $\omega_s(t)Y$ found by other authors [7] in different but related contexts.

We notice, however, that the true Regge contribution is the second term in eq. (3.27), which is of strong-coupling type, with a t-independent and eventually leading exponent $\omega_{\mathbb{P}}$. The perturbative part, which dominates in the large-t limit, comes from the background integral and has no reason to be Regge behaved.

Thus, the appearance of the parameter $\bar{\alpha}_s^5 Y^3$ is eq. (3.32) signals just the existence of a "quantum" wavelength in the solution for $\omega \lesssim \omega_s(t)$. When $\bar{\alpha}_s^5 Y^3 \sim 1$ the saddle point breaks down and the solution enters the small-t regime.

It is non-trivial, however, that in the well-defined intermediate regime (3.26), the exponent $\omega_s(t)$ with the corrections (3.32), appears to be an observable quantity. On the other hand, the exponent $\omega_c(t)$ — the formal anomalous dimension singularity in the definition (3.19) — does not directly appear in the Y dependence, because the oscillating behaviour of the $\mathcal{F}$'s is masked by the onset of $\omega_{\mathbb{P}}$ dominance for

$$Y > Y_t \equiv \frac{1}{\omega_{\mathbb{P}} - \omega_s(t)}t. \tag{3.33}$$

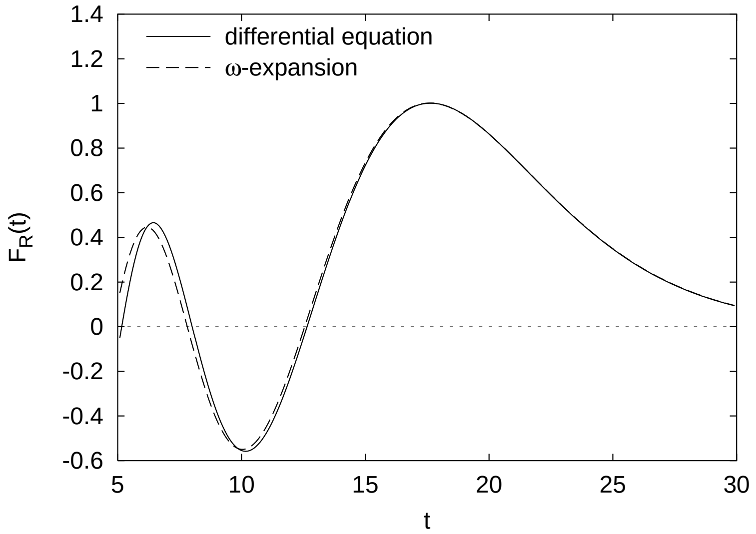

Figure 4: Regular (unintegrated) solution from the explicit solution of the differential equation and from the ω-expansion; shown for $\omega = 0.15$.

We conclude from eqs. (3.22) and (3.27) that the two-scale Green's function shows a perturbative (non-Regge) regime where the exponent $\omega_s(t)Y$ shows up with calculable corrections (eq. (3.32)), provided the parameter $\bar{\alpha}_s^5 Y^3$ is small. Even before the latter gets large, at $Y \gtrsim Y_t$ the Pomeron-dominated regime takes over, characterised by the regular solution, which is confined to the strong-coupling region of small t's.

4. Numerical results

Here we concentrate on a couple of numerical aspects. Firstly, the direct calculation in t-space of the regular solution: this permits a test of the small-ω expansion method used for the full small-x equation [11]. Secondly, the direct evolution in Y space of the Green's function, in a simplified case where the ω and A_1 dependences are removed: this allows us to elucidate the transition region between the two asymptotic regimes just mentioned.

4.1 Regular solution

First we illustrate the form of the unintegrated distribution in fig. 4, normalised to be 1 at the maximum. Results are shown both from a direct solution of the differential equation and from the ω-expansion. One sees that for larger values of t, the ω-expansion is in good agreement with the exact solution, while for smaller t, where the solutions oscillate the results from the ω-expansion are slightly out of phase with the exact solution. In general we are interested in the behaviour to the right of the rightmost zero.

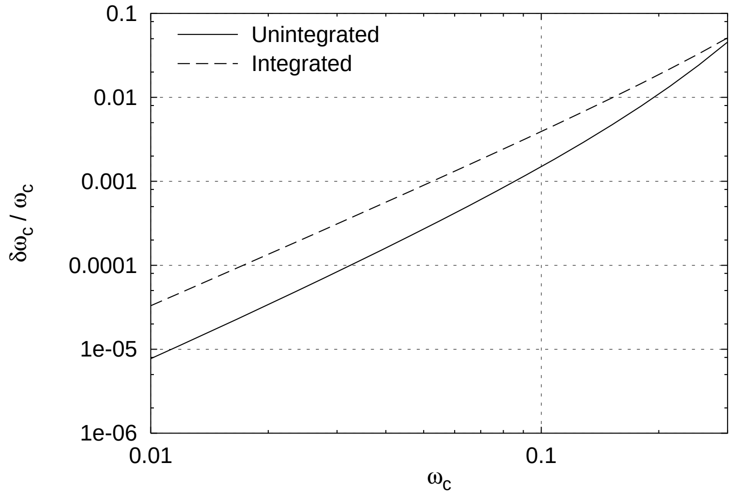

Figure 5: The error, $\delta\omega_c$ in the determination of ω_c within the ω-expansion. Shown for both the unintegrated and integrated solutions.

Critical exponent. One quantitative test of the ω-expansion concerns the critical exponent ω_c, i.e. value of ω at which the effective anomalous dimension of eq. (3.19) diverges. We recall that this is connected with the position of the rightmost zero of the regular solution: $\mathcal{F}_{\omega_c}(t) = 0$. The ω-expansion determination of the position of this zero, or equivalently its determination of ω_c as a function of t, involves a small error which we call $\delta\omega_c$. Fig. 5 shows $\delta\omega_c/\omega_c$ as a function of ω_c, and we see that the relative error on ω_c goes roughly as ω^2, or equivalently as $\bar{\alpha}_s^2$. This corresponds to a NNL correction and is beyond our level of approximation. We note also that even for relatively large values of $\omega \sim 0.3$, the relative correction remains of the order of 5% which is quite acceptable. In other words the NNL correction that arises is not accompanied by a large coefficient.

Anomalous dimensions. Our second quantitative test of the ω-expansion concerns the anomalous dimension γ, as defined in eq. (3.19). The error in the ω-expansion result for the anomalous dimension, $\delta\gamma$, is plotted in fig. 6 as a function of $\bar{\alpha}_s$ for two values of ω. Let us first concentrate on the region for $\bar{\alpha}_s < 0.01$. We see that the error is roughly independent of ω, and proportional to $\bar{\alpha}_s^2$. In other words the difference between the exact result and the ω-expansion is a term of $\mathcal{O}(\bar{\alpha}_s^2)$. We recall that the terms that we wish to include properly are the leading terms $(\bar{\alpha}_s/\omega)^n$, the NL terms $\bar{\alpha}_s(\bar{\alpha}_s/\omega)^n$ and the collinear terms $(\bar{\alpha}_s/\omega)\omega^n$. A first correction of $\mathcal{O}(\bar{\alpha}_s^2)$ is consistent with all these terms having been correctly included.

For $\bar{\alpha}_s > 0.01$ we see that the error in the anomalous dimension has a more complicated behaviour: it changes sign (the dip) and then diverges, at the same point as the divergence in the anomalous dimension itself (solid curve): this is just a consequence of the position of the divergence of the anomalous dimension from the ω-expansion being slightly different from the true position (cf. fig. 5).

JHEP10(1999)017

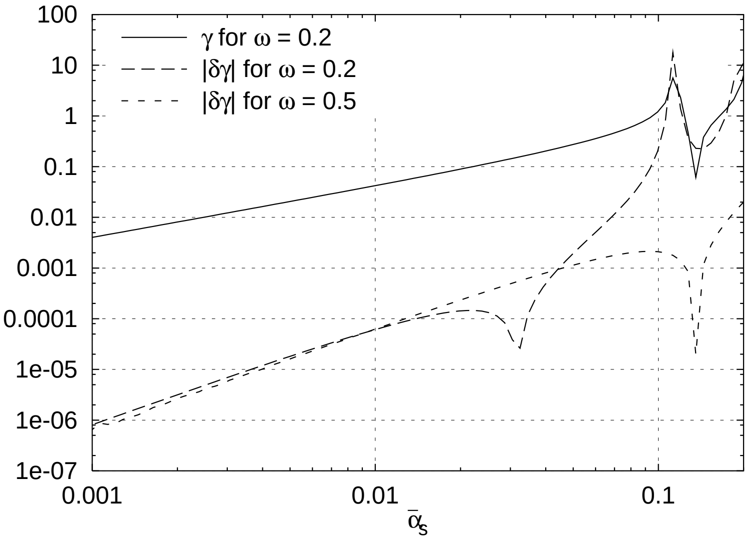

Figure 6: Error in the effective anomalous dimension of eq. (3.19) from the ω-expansion plotted against $\alpha_s(t)$.

4.2 Green's function with running coupling, diffusion, the infra-red

We have already discussed in sect. 3.3 the analytical expression for the Green's function of our model, and the features of the perturbative and strong-coupling regimes in the Y-dependence. Here we want to study the transition region between the two, which is analytically hard to describe.

Note first that several aspects of the regimes are due to just running α_s effects. The latter enters at two levels: first, because of the "acceleration" in the well of fig. 2, it modifies the traditional fixed-α_s kind of diffusion, weighting it towards lower transverse scales — this may well be connected with the breakdown of the saddle-point approximation for $\alpha_s^{5/3}Y \sim 1$ as discussed above. Secondly, because of the strong-coupling boundary condition, it also introduces a qualitatively new kind of diffusion, perhaps more properly referred to as 'tunneling': namely there is a certain $Y = Y_t$, defined in eq. (3.33), at which the non-perturbative pomeron suddenly takes over, because

$$e^{\omega_{\mathbb{P}}Y - t} \gtrsim e^{\omega_s(t)Y} \tag{4.1}$$

and beyond which the Green's function is dominated by the regular solution, and thus confined to small t-values.

This 'tunneling' phenomenon is qualitatively different from diffusion, in so far as there is not a gradual decrease in the relevant scale for the evolution, until non-perturbative scales become important, but rather there is a point beyond which low scales suddenly dominate, without intermediate scales ever having been relevant. To see this consider that the contribution to the evolution at scale t from an intermediate scale $t_i \ll t$ (with a corresponding exponent $\omega_i \simeq \chi_m/bt_i$), is of order

$$e^{\chi_m Y/(bt_i)-(t-t_i)}\,. \tag{4.2}$$

From this one sees, because of eq. (4.1), that $t_i = \bar{t}$ becomes relevant before higher scales do.

To study these effects at a qualitative level it suffices to consider a very simplified version of the collinear model: one which retains only the running of the coupling, but not the ω-shifts of the $\gamma = 0, 1$ poles, nor the A_1 component of the NL corrections. We then examine the solution to

$$\mathcal{G}(Y,t,t_0) = \delta(t-t_0) + \int_0^Y \mathrm{d}y\; K \otimes \mathcal{G}(y)\,, \tag{4.3}$$

for this simplified kernel and we consider the effective exponent of the evolution

$$\omega_{\mathrm{eff}} = \frac{\mathrm{d}}{\mathrm{d}Y} \ln \hat{\mathcal{G}}(Y,t,t) \tag{4.4}$$

as a function of Y, where $\hat{\mathcal{G}}(Y,t,t_0)$ is simply $\mathcal{G}(Y,t,t_0)$ with $\delta(t-t_0)$ subtracted, in analogy with eq. (2.33). Fig. 7 illustrates the basic behaviour of ω_{eff} for rather extreme kinematics — not intended to be phenomenologically relevant, but rather to show clearly the relevant features. Two values of the infra-red cutoff are considered. What is seen is that the exponent at first increases slowly and smoothly, and then at a certain threshold Y increases rapidly towards $\omega_{\mathbb{P}}$. The saturation of $\omega_{\mathbb{P}}$ occurs later in Y for increased $\bar{t}$ (i.e. decreased $\omega_{\mathbb{P}}$) as expected from (3.33). Traditional smooth diffusion into the infra-red would have led to the opposite behaviour, namely the higher $\bar{t}$ case (lower $\omega_{\mathbb{P}}$) being saturated first.

The study of traditional diffusion is a little trickier, essentially because for most parameter choices there is only a limited domain of traditional diffusion before tunneling takes over. Nevertheless one way to approach it is to study the difference between the effective exponents in a case with running α_{s} and one with fixed α_{s}. For this comparison to be meaningful the fixed α_{s} must be chosen such that $\alpha_{\mathrm{s}}\chi_0(1/2) = \omega_s(t)$. The observed difference in exponent is then a measure of the difference in the diffusion properties of the running and fixed-α_{s} cases: it is sensitive to the terms which are expected to be sizeable when $\alpha_{\mathrm{s}}^5 Y^3 \sim 1$.

The difference is shown in fig. 8, where the dashed line is based on eq. (3.32), which in turn reproduces the results by Kovchegov and Mueller and by Levin [7] (with the proper changes for the χ_m and χ_m'' values). The agreement is good, up to the critical value Y_t beyond which the Pomeron regime takes over.

In fig. 8 we have taken extreme values of t and Y, in order to identify the running coupling corrections, and we have thus emphasised the difference $\omega_{\mathbb{P}} - \omega_s(t)$ also. With realistic parameters and model, the transition between the two regimes could be smoother and shifted to relatively higher energies.

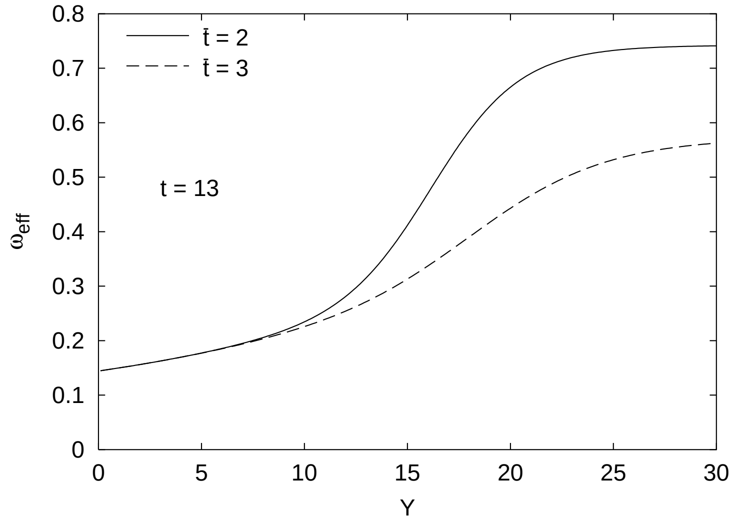

Figure 7: The effective intercept ω_{eff} as a function of Y for $t = 13$ and two different values of the infra-red cutoff $\bar{t}$.

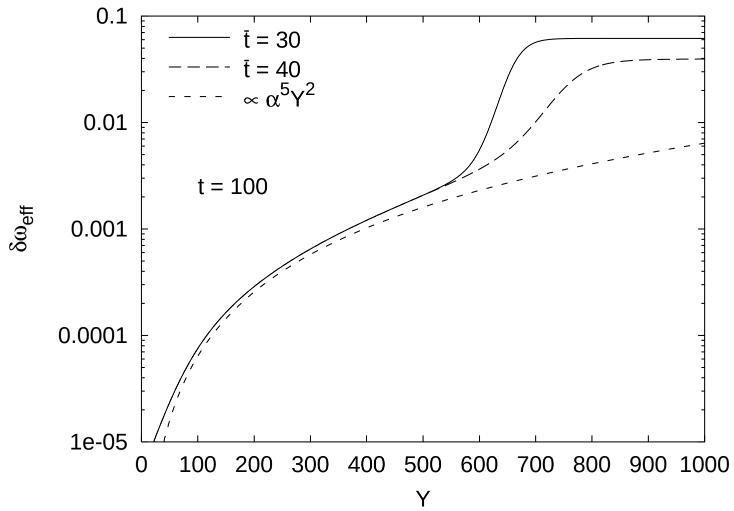

Figure 8: The difference $\delta\omega_{\text{eff}}$ between the effective exponents seen with running $\bar{\alpha}_{\text{s}}$ and fixed $\bar{\alpha}_{\text{s}}$ $(= 1/101)$, shown for two values of $\bar{t}$. Shown for very extreme values of t and Y in order to expose more clearly the main features.

5. Discussion

The model that we have introduced is somewhat intermediate between the full RG-improved small-x equation and the (Airy) diffusion model with running coupling. Compared to the latter, it has the advantage of a correct collinear behaviour, while still admitting a Schrödinger-type treatment. It appears, therefore, as a useful laboratory for testing approximation methods and theoretical prejudices.

We have already performed several tests. First, we have shown (sect. 4.1) that the ω-expansion of the γ-representation indeed provides a quite good approximation

JHEP10(1999)017

of the regular solution, which is thus perturbative, i.e., independent of the boundary conditions in the strong-coupling region. This lends further support to previous results [11] on the anomalous dimensions and the hard Pomeron.

We have further used the present model to analyse the gluon Green's function, by testing its factorisation properties, and by providing its explicit expression (sect. 3) which involves the left-regular solution, and is thus dependent on the strong-coupling region. In the present model, this dependence occurs through a single scattering coefficient $S(\omega)$, which carries the spectrum and thus the leading Pomeron singularity (eq. (3.5)). It is expected, by the arguments of ref. [16], that a similar decomposition may be valid in general, perhaps with several scattering coefficients.

For two-scale processes, the results of sects. 3.3 and 4.2 are of particular interest: in an intermediate Y region a perturbative regime exists where the exponent $\omega_s(t)$ is observable, with corrections of type $\bar{\alpha}_s^5 Y^3$, whose size is in agreement with refs. [7]. On the other hand, for large enough energies, $Y \gtrsim t/(\omega_{\mathbb{P}} - \omega_s(t))$, the Regge behaviour due to the non-perturbative Pomeron takes over with a "tunneling" transition to small t's which may, in principle, be spectacular for sizeable values of $\omega_{\mathbb{P}} - \omega_s(t)$.

Several points need further elucidation. First, a realistic evaluation of $\omega_{\mathbb{P}}$ and of the related effective coupling is still needed, in order to put the question of the regimes in perspective, and to start making predictions for two-scale processes. In particular, the size of $\omega_{\mathbb{P}}$ (including possible unitarity corrections) seems to be crucial in order to understand how fast and experimentally relevant is the transition to the Pomeron regime.

Furthermore, the relative importance of the perturbative exponents $\omega_s(t)$ and $\omega_c(t)$ and of $\omega_{\mathbb{P}}$ is still to be cleared up in DIS-type processes, where t-evolution plays a much more important role.

For all these questions the present model is likely to provide useful hints and a preliminary understanding.

Acknowledgments

One of us (G.P.S.) wishes to acknowledge stimulating conversations with Raju Venugopalan on issues related to diffusion and running coupling.

References

[1] L.N. Lipatov, *Sov. J. Nucl. Phys.* **23** (1976) 338;
E.A. Kuraev, L.N. Lipatov and V.S. Fadin, *Sov. Phys. JETP* **44** (1976) 443; *Sov. Phys. JETP* **45** (1977) 199;
Ya. Balitskii and L.N. Lipatov, *Sov. J. Nucl. Phys.* **28** (1978) 822.

[2] L.N. Lipatov and V.S. Fadin, *Sov. J. Nucl. Phys.* **50** (1989) 712;
V.S. Fadin, R. Fiore and M.I. Kotsky, *Phys. Lett.* **B 359** (1995) 181; *Phys. Lett.* **B**

387 (1996) 593 [hep-ph/9605357];
V.S. Fadin, and L.N. Lipatov, *Nucl. Phys.* **B 406** (1993) 259;
V.S. Fadin, R. Fiore and A. Quartarolo, *Phys. Rev.* **D 50** (1994) 5893 [hep-th/9405127];
V.S. Fadin, R. Fiore, and M. I. Kotsky, *Phys. Lett.* **B 389** (1996) 737 [hep-ph/9608229];
V.S. Fadin and L.N. Lipatov, *Nucl. Phys.* **B 477** (1996) 767 [hep-ph/9602287];
V.S. Fadin, M.I. Kotsky and L.N. Lipatov, *Phys. Lett.* **B 415** (1997) 97 [hep-ph/9704267];
S. Catani, M. Ciafaloni and F.Hautman, *Phys. Lett.* **B 242** (1990) 97; *Nucl. Phys.* **B 366** (1991) 135;
V. S. Fadin, R. Fiore, A. Flachi, and M. I. Kotsky, *Phys. Lett.* **B 422** (1998) 287 [hep-ph/9711427].

[3] V.S. Fadin and L.N. Lipatov, *Phys. Lett.* **B 429** (1998) 127 [hep-ph/9802290].

[4] M. Ciafaloni and G. Camici, *Phys. Lett.* **B 412** (1997) 396 [hep-ph/9707390];
M. Ciafaloni, *Phys. Lett.* **B 429** (1998) 363 [hep-ph/9801322];
M. Ciafaloni and G. Camici, *Phys. Lett.* **B 430** (1998) 349 [hep-ph/9803389].

[5] J. Blümlein, W.L. van Neerven, V. Ravindran and A. Vogt, *The unpolarized gluon anomalous dimension at small x*, hep-ph/9806368;
J. Blümlein, W.L. van Neerven and V. Ravindran, *Phys. Rev.* **D 58** (1998) 091502 [hep-ph/9806357].

[6] D.A. Ross, *Phys. Lett.* **B 431** (1998) 161 [hep-ph/9804332].

[7] Yu.V. Kovchegov and A.H. Mueller, *Phys. Lett.* **B 439** (1998) 428 [hep-ph/9805208];
E. Levin, *The BFKL high energy asymptotics in the next-to-leading approximation*, hep-ph/9806228.

[8] G.P. Salam, *J. High Energy Phys.* **07** (1998) 019 [hep-ph/9806482].

[9] M. Ciafaloni and D. Colferai, *Phys. Lett.* **B 452** (1999) 372 [hep-ph/9812366].

[10] R.S. Thorne, *Phys. Rev.* **D 60** (1999) 054031 [hep-ph/9901331].

[11] M. Ciafaloni, D. Colferai and G.P. Salam, *Renormalization group improved small-x equation*, hep-ph/9905566.

[12] H1 collaboration, *Z. Physik* **C 72** (1996) 593 [hep-ex/9607012];
ZEUS collaboration, *Phys. Lett.* **B 407** (1997) 402 [hep-ex/9706009].

[13] L3 collaboration, *Phys. Lett.* **B 453** (1999) 333.

[14] ZEUS collaboration, *Eur. Phys. J.* **C 6** (1999) 239 [hep-ex/9805016];
H1 collaboration, *Nucl. Phys.* **B 538** (1999) 3 [hep-ex/9809028].

[15] V.N. Gribov and L.N. Lipatov, *Sov. J. Nucl. Phys.* **15** (1972) 438;
G. Altarelli and G. Parisi, *Nucl. Phys.* **B 126** (1977) 298;
Yu.L. Dokshitzer, *Sov. Phys. JETP* **46** (1977) 641.

[16] G. Camici and M. Ciafaloni, *Phys. Lett.* **B 395** (1997) 118 [hep-ph/9612235].

[17] L.V. Gribov, E.M. Levin and M.G. Ryskin,*Phys. Rep.* **100** (1983) 1.

[18] J. Kwiecinski, *Z. Physik* **C 29** (1985) 561;
J.C. Collins and J. Kwiecinski, *Nucl. Phys.* **B 316** (1989) 307.

[19] J. Bartels and H. Lotter, *Phys. Lett.* **B 309** (1993) 400.

[20] see, e.g., J.R. Forshaw and D.A. Ross, *Quantum chromodynamics and the pomeron*, Cambridge University Press, 1997.

[21] M. Abramowitz and I. Stegun, *Handbook of mathematical functions*, Dover Publication, New York 1965.